

Analysis of small-angle scattering of polarized neutrons in unmagnetized ferroliquids

L. A. Aksel'rod, G. P. Gordeev, G. M. Drabkin, I. M. Lazebnik, and V. T. Lebedev

Leningrad Institute of Nuclear Physics, USSR Academy of Sciences

(Submitted 16 October 1985; resubmitted 17 February 1986)

Zh. Eksp. Teor. Fiz. **91**, 531–541 (August 1986)

Low-angle scattering of polarized neutrons in ferroliquids in the absence of an external magnetic field is studied. The liquids are stable suspensions of like particles of magnetite in kerosene (volume concentrations of the magnetite $C \approx 0.45, 0.04, 0.02, 0.01, 0.005$, and 0.0025). The contributions of magnetic and nuclear scattering to the total scattering cross sections are determined, and their dependences on the momentum transfer are analyzed. It is shown that the magnetic moments of the particles correlate in direction over considerable distances. On the other hand, no spatial correlations of the particles were observed. The correlations of the magnetic moments vanish below a definite concentration. The dimensions of the inhomogeneities are estimated. Inelastic neutron scattering was also observed and permitted an estimate of the characteristic times of the processes ($\sim 10^{-11}$ s).

1. INTRODUCTION

Stable suspensions of minute ferromagnetic particles of the same kind, called ferroliquids (FL), are being intensely investigated of late. The causes are, first, the general interest in physics of disordered systems, and second, the many practical uses of ferroliquids.¹⁾ An appreciable part of the papers devoted to these liquids deal with investigations of their structure.

A distinguishing feature of the structure of a magnetic suspension is aggregation of the particles in an external magnetic field, as observed in various FL²⁻⁷ and predicted theoretically.⁸⁻¹² At present, however, there is no meeting of mind concerning the structure of such aggregates. Stable configurations of the aggregates in a magnetic field can be either linear chains⁸⁻¹¹ oriented along the field \mathbf{H} or more massive formations.¹² Although no aggregates were observed in the aforementioned experiments after the magnetic field was turned off, there are nevertheless weighty indications that aggregation does take place also in a zero field.^{8,11,13} One of the causes is the long-range action of the dipole forces. If the average energy of the magnetodipole interaction of the particles is high enough to meet the condition

$$m^2/r^3 \gg k_B T$$

(m is the average magnetic moment of the particle, r the average distance between particles, T the temperature, and k_B Boltzmann's constant), the moments of the particles may turn out to be correlated by the internal field $H_i \propto mn$ (n is the particle concentration). The energy of this field may be sufficient to maintain a local polarization of the FL, and this will affect also the relative positions of the particles (spatial correlation).

No systematic experimental study of the correlations in FL in the absence of a field has been made so far. The reason is that magnetic fields are usually employed in one way or another in investigations of the FL structure and inevitably

upset the initial state of the liquid. We have therefore used in the present study a nonperturbing method, viz., small-angle scattering of polarized neutrons. Measurement of the scattering intensity and simultaneous analysis of the polarization of the scattered beam has made it possible to separate the contributions of the magnetic and nuclear resonances to the total cross sections, and estimate by the same token the sizes of the scattering inhomogeneities, both magnetic and nuclear, in suspensions, stabilized with oleic acid, of magnetite in kerosene. The magnetic dimension was determined also independently of the measured depolarization of the polarized neutron beam passing through the FL samples. In addition, we have observed inelastic scattering of the neutrons, which casts light on the dynamics of the FL particles.

2. METHOD OF SEPARATING THE MAGNETIC AND NUCLEAR CROSS-SECTION COMPONENTS

On the whole, an unmagnetized FL can be regarded as a paramagnet in which magnetic scattering and coherent and incoherent nuclear scattering of neutrons take place. The incoherent nuclear scattering is due to the hydrogen of the liquid medium (kerosene and oleic acid in this case). Thus, the measured scattering cross section is the sum of cross sections of the following contributions:

$$\frac{d\sigma_e(q)}{d\Omega} = \sum_j \frac{d\sigma_j(q)}{d\Omega}, \quad (1)$$

where \mathbf{q} is the scattering cross section; $\mathbf{q} = \mathbf{k} - \mathbf{k}_0$; \mathbf{k}_0 and \mathbf{k} are the initial and final neutron wave vectors, and the subscript j stands for coherent nuclear (nc) magnetic (m) and incoherent (inc) cross sections. If the neutrons are polarized, the resultant polarization vector after scattering is¹⁴

$$\mathbf{P}_e(q) = \left(\sum_j \mathbf{P}_j(q) \frac{d\sigma_j(q)}{d\Omega} \right) \left(\sum_j \frac{d\sigma_j(q)}{d\Omega} \right)^{-1}, \quad (2)$$

where $\mathbf{P}_j(q)$ are the polarization vectors corresponding to the various contributions to the scattering. Transforming

from cross sections to intensities $I_j(q)$ and recognizing that background neutrons, having their own polarization $\mathbf{P}_b(q)$ and intensity $I_b(q)$, are always present, we get in place of (1) and (2) the following balance equations:

$$\begin{aligned} P_e(q)I_e(q) &= \sum_j P_j(q)I_j(q) + P_b(q)I_b(q), \\ I_e(q) &= \sum_j I_j(q) + I_b(q). \end{aligned} \quad (3)$$

The following is known concerning the polarization vectors $\mathbf{P}_j(\mathbf{q})$. In coherent nuclear scattering by unpolarized nuclei the polarization is unchanged, i.e., $P_{nc} = P_0$, where P_0 is the polarization of the incident neutrons. For incoherent scattering by hydrogen, $\mathbf{P}_{inc} = \mathbf{P}_0/3$ and, finally for paramagnetic scattering we have¹⁵

$$\mathbf{P}_m = -c(\mathbf{eP}_0), \quad (4)$$

where $\mathbf{e} = \mathbf{q}/q$. If the magnetic small-angle scattering is elastic, only the polarization components P_{mx} and P_{my} perpendicular to the wave vector \mathbf{k}_0 are present, and the component P_{mz} parallel to \mathbf{k}_0 is zero. (It is assumed here and elsewhere that the beam is directed along the Z axis and the scattering is analyzed along the Y axis in the horizontal YZ plane). In the general case, when inelastic magnetic scattering is also present, the component P_{mx} is likewise not zero. Then, as can be seen from (4), we have the relation

$$\sum_i (P_{mi}/P_{0i}) = -1, \quad i=x, y, z. \quad (5)$$

Nothing is known beforehand concerning the background polarization $\mathbf{P}_b(q)$, nor concerning the intensity $I_b(q)$. They must be determined from experiment. Thus, measurements of the intensity and polarization of the scattered beam with \mathbf{P}_0 oriented along the three coordinate axes (X, Y, Z) make it possible to determine easily, with the aid of (3) and (5), the contributions I_{nc} , I_m , and I_{inc} of interest to us, and also the components P_{mi} . The contribution of the incoherent scattering is determined by measuring, under the same experimental conditions, the scattering from only the liquid medium: since incoherent scattering has no angular

dependence (neglecting the thermal factor), the contribution I_{inc} from the FL is proportional to the volume content of the liquid carrier in the FL sample.

3. EXPERIMENT AND GENERAL PROPERTIES OF THE EXPERIMENTAL DATA

The experiments on small-angle scattering of polarized neutrons were performed with the apparatus¹⁶ shown schematically in Fig. 1. This apparatus can produce a beam of polarized neutrons with average wavelength $\lambda = 9 \text{ \AA}$ and with deviation $\Delta\lambda/\lambda = 0.3$ from monochromatic, carry out a three-dimensional analysis of the polarization, and simultaneously measure scattering at 20 angles θ and analyze the polarization of the scattered beam. To this end, a special unit in the apparatus can orient the initial-polarization vector \mathbf{P}_0 along the coordinate axes and analyze the corresponding projections $P_{ei}(q)$ of the scattering-beam polarization vector $\mathbf{P}_e(q)$. Twenty detectors contained in a single block subtend an angle $\theta_n = 4.5^\circ$. The vertical angle of each detector is $\sim 1^\circ$, and the horizontal $\sim 14'$. An analyzing mirror is placed in front of each detector.

The depolarization of a monochromatic beam with $\lambda = 2.3 \text{ \AA}$ ($\Delta\lambda/\lambda = 0.02$) passing through the FL was measured with apparatus functionally analogous to that of Fig. 1. The beam was made monochromatic by using a strained germanium crystal.

The samples were suspensions of magnetite particles in kerosene, with a solid-phase volume concentration $C \approx 0.45, 0.04, 0.02, 0.01, 0.005,$ and 0.0025 . A surface-active substance, oleic acid, was added in the suspension-preparation stage. The average magnetite particle dimension (from magnetic measurements) was of the order of 120 \AA with a spread 25–30%. In the measurements, the FL was placed in a planar quartz ampule. The liquid-layer thickness was 2 mm (10 mm in the depolarization measurements). The same ampule was used to measure the scattering from the kerosene with oleic acid so as to determine the contribution of the nuclear incoherent scattering. The polarization of the beam scattered by the empty ampule was taken to be $P_b(q)$, and its intensity, decreased by the attenuation of the sample, was taken to be $I_b(q)$.

The field at the sample was $\sim 0.5 \text{ Oe}$, i.e., $\sim 2 \cdot 10^{-3}$ of

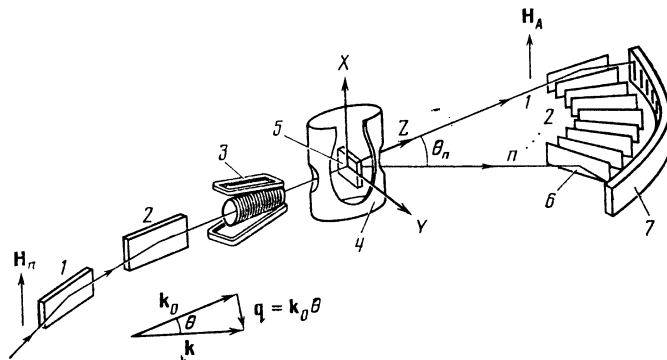


FIG. 1. Diagram of small-angle-scattering apparatus: 1—polarizing mirror, 2—mirror to filter the γ rays and the fast neutrons out of the beam, 3—adiabatic rf flipper, 4—screen of vector analyzer of the polarization, 5—sample, 6—multichannel analyzer, 7—multi-channel detector, 8—scattering angle, n —number of detector channel, θ_n —maximum angle subtended by detector block. The arrows \mathbf{H}_n and \mathbf{H}_A show the magnetization directions of the polarizer and analyzer.

the saturation field of a FL with concentration 0.04. Even in the strongly concentrated (paste-like) FL ($C \approx 0.45$) such a field does not disturb noticeably the isotropy of the medium. This was verified by measuring the polarization of a transmitted beam with the orientations of the vector \mathbf{P}_0 relative to the neutron-velocity vector. It is known¹⁷ that neutron beams polarized parallel and perpendicular to the vector \mathbf{k}_0 in a medium with distributed magnetic inhomogeneities (domains, clusters, fluctuations) becomes depolarized in a ratio

$$\frac{\ln(P_{\perp}/P_{0\perp})}{\ln(P_{\parallel}/P_{0\parallel})} = \frac{3}{2}.$$

For an essentially anisotropic distribution, the depolarization ratio differs from 3/2. Depending on the character of the anisotropy, this reaction is either larger or smaller by several times.¹⁸ We have observed a decrease in a range of 10% ($C \approx 0.45$), and took the 0.5-Oe field to be practically zero for the investigated FL.

The procedure of resolving the total cross section into components was initially verified for the FL sample with large (0.45) particle concentration, since it had a large magnetic and nuclear scattering ability. Small-angle scattering and all the other necessary measurements were performed in this case with a narrower beam than for sufficiently diluted FL. For a qualitative comparison with the data for low concentrations, we shall present below also the data for this high one.

The experimental data for the intensity $I_e(q)$ and polarization $P_{ei}(q)$ are shown in Fig. 2.²⁾ The following properties are noteworthy: 1) The nonmonotonic scattering curve $I_e(q)$ for $C \approx 0.45$ (Fig. 2a), a consequence of the high particle density. 2) the change of the character of the scattering intensity as a function of concentration at small volume concentrations (curves 5 and 6); possible explanations of this fact are given in Sec. 4 below. 3) The magnetic scattering is concentrated in the region of small momentum transfers, as can be seen from the $P_{ei}(q)$ plots (Fig. 2b). The contribution of scattering with spin flip is a maximum in the region $q < 3 \cdot 10^{-2} \text{ \AA}^{-1}$. In a low-concentration FL the magnetic scattering is substantially smaller than the nuclear, so that the polarization level is quite high.

Figure 2 shows also the background data $I_b(q)$ (Fig. 2a) and $P_b(q)$ (Fig. 2b), as well as the maximum I_b level corresponding to the FL with the lowest concentration ($C = 0.0025$).

Information on incoherent scattering was obtained from measurements of scattering by kerosene with oleic acid (Fig. 3a). The incoherent scattering intensity I_{inc}^{ker} (Fig. b), as expected, is independent of q , and the mean value of P_{inc}^{ker} (dashed line in Fig. 3b) equals $-1/3$ within the error limits.

4. DISCUSSION OF RESULTS

1. Analysis of cross sections for nuclear and magnetic scattering

The nuclear $I_{nc}(q)$ and magnetic $I_m(q)$ components of the total cross section are shown in Figs. 4 and 5, respectively.

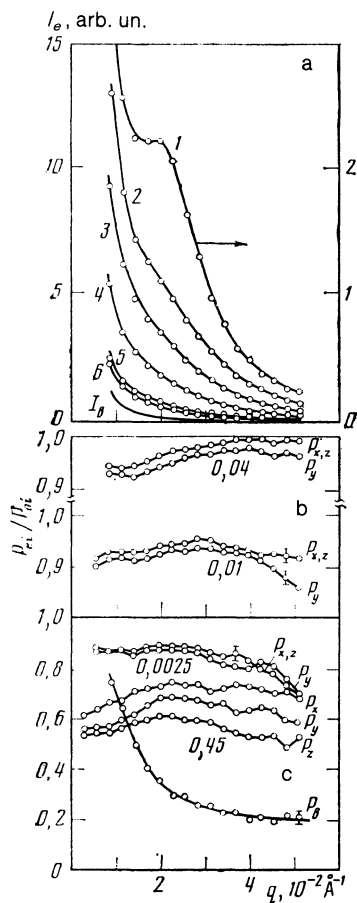


FIG. 2. Experimental small-angle scattering data; a—scattering intensity $I_e(q)$ and background intensity $I_b(q)$. The magnetite concentrations for the $I_e(q)$ curve are: 1—0.45; 2—0.04; 3—0.02; 4—0.01; 5—0.0025; 6—0.005. The intensity $I_b(q)$ is indicated for $C = 0.0025$; b—polarization P_{ei} normalized to the initial P_{0i} ($i = x, y, z$), and background polarization P_b . The volume concentration of the magnetite is indicated for each group of curves.

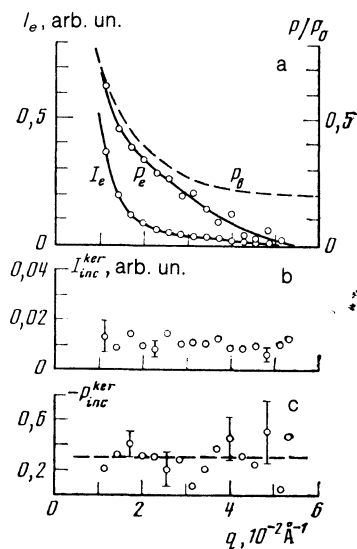


FIG. 3. Scattering by kerosens with oleic acid: a—experimental data for the scattering intensity and polarization; the dashed line shows the background polarization; b—intensity and polarization, respectively, of the incoherent scattering, reconstructed from the experimental data.

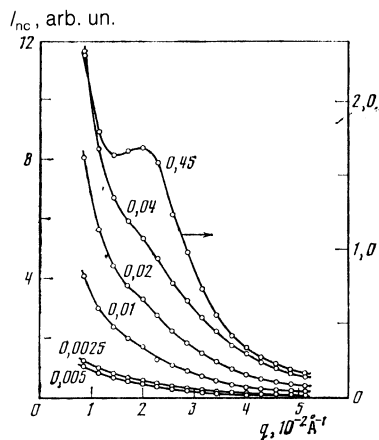


FIG. 4. Nuclear scattering intensity $I_{nc}(q)$. The corresponding volume concentrations of the magnetite are marked on the curves.

The properties of the total cross section, noted in the preceding section, are manifested to a greater degree in the nuclear-scattering cross section. The magnetic scattering has a monotonic dependence on the momentum transfer. It has the same intensity, within the limit of statistical accuracy, at the concentrations 0.005 and 0.0025. The magnetic scattering is weaker than nuclear by a factor 40–50 and decreases with increasing q more rapidly. The rate of the decrease depends on the concentration. This is clearly illustrated in Fig. 6, where $I_{nc}(q)$ and $I_m(q)$ for each concentration are normalized to the corresponding value at $q = 1.15 \cdot 10^{-2} \text{ \AA}^{-1}$. The nuclear-scattering curves, which are contained in band I, decrease more slowly than the magnetic-scattering curves, which are bunched for the most part in band II. At concentrations lower than 0.01, the curves show a tendency to “cross over” from band II to band I, and then the $I_m(q)$ curves corresponding to the concentrations 0.005 and 0.0025 land in band I.

It can be concluded from this qualitative analysis that the nuclear density of the scatterers is spatially more compact than the magnetic. In other words, this may mean that the magnetic moments are correlated over distances larger than the particle size. The weakly pronounced interference

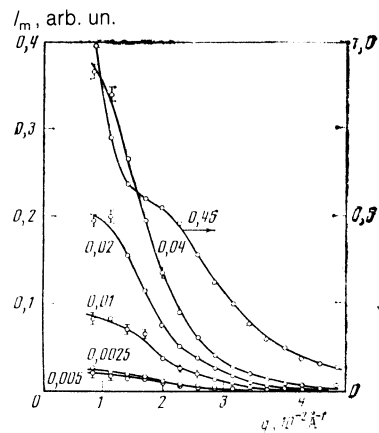


FIG. 5. Intensity $I_m(q)$ of magnetic scattering. The corresponding magnetite concentrations are marked on the curves.

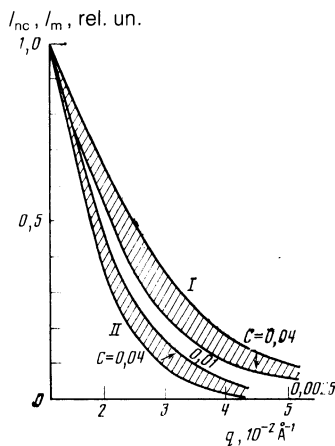


FIG. 6. Qualitative comparison of the nuclear (I_{nc}) and magnetic (I_m) scattering. The intensities are normalized to the value at $q = 1.15 \times 10^{-2} \text{ \AA}^{-1}$. I—interval of I_{nc} values for the range $C = 0.04$ – 0.0025 and of I_m for $C = 0.005$ and 0.0025 ; II—interval of I_m for $C = 0.04, 0.02, \text{ and } 0.01$. The arrows point towards decreased concentrations.

pattern in magnetic scattering attests to a broad distribution of the magnetic dimensions.

2. Estimate of magnetic and nuclear dimensions

Unfortunately, a quantitative analysis of small-angle scattering meets with difficulties when it becomes an analytic description of the experimental data. The use of the Guinier approximation¹⁹ for the scattering functions $I_{nc}(q)$ and $I_m(q)$ is irrelevant in this case, since the conditions for its validity (identity of the particles, strong dilution, absence of correlations) are, generally speaking, not met here. Yet it is known²⁰ that the $1/q^4$ law is satisfied in a number of cases for the scattering-curve wings, regardless of the degree of dilution of the system and of the spread of the scatterer sizes.

In this case, the asymptotics of scattering curves $I_m(q)$ and $I_{nc}(q)$ are such that the reciprocal intensities $1/I_{nc}$ and $1/I_m$ become proportional to q^4 (Fig. 7). Extrapolation to $q = 0$ gives the intercepts on the reciprocal-intensity axes. The reciprocal intensities $1/I_j(0)$ were used thereafter to estimate the magnetic and nuclear dimensions of the scatterers, by changing over from intensities to absolute cross sections and by comparison with the known expressions $d\sigma_{nc}/d\Omega$ and $d\sigma_m/d\Omega$ at $q = 0$.

The change to absolute cross section was made by normalization to the cross section for incoherent scattering in the given FL:

$$\frac{d\sigma_j}{d\Omega} = \frac{I_j(q)}{I_{inc}(q)} \frac{d\sigma_{inc}}{d\Omega}, \quad (6)$$

where I_{inc} is the incoherent-scattering intensity. For a hydrogen-containing medium,

$$d\sigma_{inc}/d\Omega = a^2 N_p, \quad (7)$$

where a is the amplitude for scattering by a proton and N_p is the number of protons.

We regarded FL with concentrations $C = 0.04$ – 0.0025 as dilute, and used therefore the most general expression for the cross section for small-angle neutron scattering by a sys-

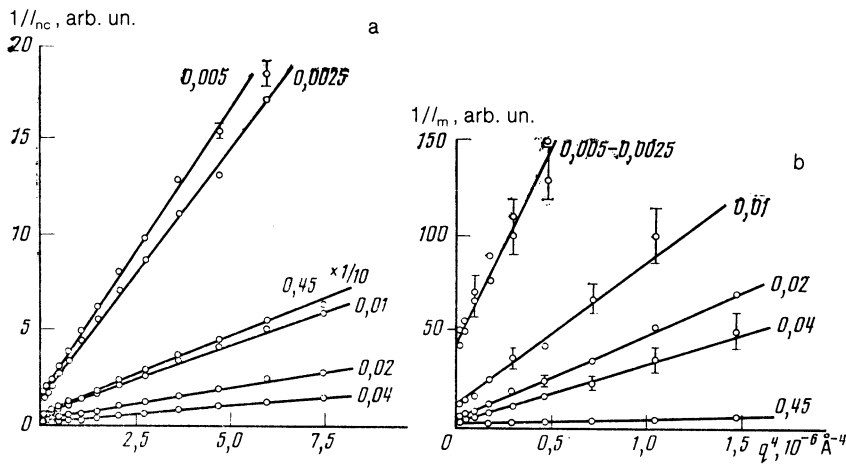


FIG. 7. Reciprocal of intensity vs q^4 for nuclear (a) and magnetic (b) scattering.

tem of N particles that are sufficiently distant from one another at $q = 0$:

$$d\sigma_{nc}/d\Omega = K^2 N V_{nc}^2, \quad (8)$$

where V_{nc} is the nuclear (physical) volume of the particle, $K = a_1/V_1 - a_2/V_2$ is the contrast factor, a_1 and a_2 are the amplitudes of the nuclear scattering of magnetite and kerosine molecules, and V_1 and V_2 are the volumes of their molecules.

To describe magnetic scattering we used the paramagnetic-scattering formula¹⁴ at $q = 0$:

$$d\sigma_m/d\Omega = \frac{2}{3} (\gamma r_0)^2 S^2 N_m, \quad (9)$$

where γ is the magnetic moment of the neutron in nuclear magnetons, r_0 is the classical radius of the electron, $S = MV_m/g\mu_B$ is the total spin of the scattering inhomogeneity and is connected with its magnetization M and its volume $V_m \cdot \mu_B$ is the Bohr magneton, g is the Lande factor, and N_m is the number of "magnetic" scatterers. We have thus obtained from (8) and (9), with account taken of (6) and (7), the respective volumes V_{nc} and V_m . It is more convenient to use in place of the volumes the characteristic particle dimensions, which are of the order of $V^{1/3}$. The parameters d_n and d_m were determined by using the condition for normalization to the bulk concentration of the magnetic phase, viz., $N_m V_m = n V_0 \equiv C$ (n is the density of the "elementary" magnetic-moment carriers of volume V_0). This condition is exact for the nuclear dimensions. As for the magnetic dimen-

sions, the condition is valid only for inhomogeneities consisting of dipoles with parallel moments. The FL definitely contain inhomogeneities with antiparallel orientation of the moments (side by side), so that their volume $V_m = 0$. Since these inhomogeneities do not contribute to the magnetic scattering at $q = 0$, it would be necessary to take them into account when d_m is determined. For lack of a correct method for such an account, we have neglected them completely, so that the indicated values of d_m are lower bounds of the dimensions for parallel orientations of the moments. These dimensions are listed in Table I.

In the calculation of the magnetic dimension d_m we used the value $M = 400$ G, estimated from the saturation magnetization of magnetite. Another independent method of determining magnetic dimensions was to measure the depolarization of a beam of neutrons with $\lambda = 2.3$ Å passing through the sample. It is known¹⁷ that depolarization of magnets is caused by the large magnetic inhomogeneities that scatter neutrons into the detector aperture. If the initial polarization P_0 is perpendicular to the neutron velocity v , the polarization of the beam passing through the sample is given by

$$P = P_0 \exp(-\frac{3}{2} N_m \sigma_m L), \quad (10)$$

where σ_m is the cross section for scattering into the detector aperture, L is the sample thickness, and N_m is the density of the magnetic inhomogeneities (clusters, fluctuations, domains, etc.) with characteristic radius $R = d/2$. The prod-

TABLE I. Principal results of experiment.

Volume concentration of Fe ₃ O ₄	Small-angle scattering ($\bar{\lambda} = 9$ Å, $\Delta\lambda/\bar{\lambda} = 0.3$)			Depolarization ($\lambda = 2.3$ Å, $\Delta\lambda/\lambda = 0.02$)	
	d_n , Å	d_m , Å	$(\langle \omega \rangle^2 q)^{1/2}$, mkeV	P/P_0	d , Å
0.45	105±5	300±5	30	0.5920±0.0005	400±10
0.04	133±5	233±15	17	0.949±0.003	215±20
0.02	147±5	240±15	15	0.958±0.003	200±20
0.01	140±6	182±20	13	0.973±0.004	195±18
0.005	135±6	160±25	—	—	—
0.0025	170±8	240±30	—	0.982±0.002	160±20

uct in the argument of the exponential is connected with the properties of the neutron and of the medium²¹:

$$N_m \sigma_m L = \frac{1}{3} (\mu_n B / E)^2 k_0^2 R C^{1/2} L, \quad (11)$$

where $B = 4\pi M$ is the magnetic induction, E the energy of the neutrons, k_0 their wave vector, C the inhomogeneity concentration, and μ_n the magnetic moment of the neutron.

The resultant characteristic size d at $M = 400$ G is also listed in the table.

At higher concentrations, the magnetic size exceeds the nuclear, probably as a result of correlations of the magnetic-moment directions of several particles that scatter coherently. The difference between d_n and d_m vanishes at the concentration 0.005.

The tendency of d_n to grow weakly with decreasing concentration might indicate, generally speaking, spatial correlations of the particles. However, dilution should lead to weakening rather than strengthening of the correlation, the latter observed, e.g., in the behavior of d_m . Therefore the increase of d_n with decrease of the concentration is to factors other than spatial correlations of the particles, namely, to fluctuations of the particle density. In fact, let us estimate the number of particles with correlated magnetic moments, i.e., the number of particles contained in the magnetic cluster, for the extreme case of two concentrations, where d_n and d_m differ substantially ($C = 0.04$) and where they are equal within the limits of error ($C \leq 0.005$). If the real physical parameter $d_n \approx 120$ Å, the particle concentration in the first FL is $n = 4.4 \cdot 10^{16} \text{ cm}^{-3}$. The concentration of magnetic clusters of size d_m however, turns out to be $\sim 6.7 \cdot 10^{15} \text{ cm}^{-3}$. Assuming that all the particles are gathered into such clusters, we have an average of ~ 7 particles per cluster, i.e., each particle has approximately 6 neighbors that contribute to the total moment. Similar estimates for FL with lower concentrations show that this number is considerably lower, 2–3 particles per cluster on the average.

Such small particle aggregates exist also, generally speaking, at higher concentrations, but their relative contribution to the scattering is small. With decreasing concentration, their relative number increases and this increases effectively the spread of the sizes. This probably explains the small increase of the physical size d_n with decrease of the concentration, i.e., one can see in fact small fluctuations of the particle density. The formation of small aggregates is random. At high concentrations ($C > 0.005$) the probability of their formation is lower because of the influence of the random field of the closer neighbors. In other words, such aggregates are metastable, but at low concentrations they behave as stable formations. Once they collide the particles have a lower probability of moving apart in view of the absence of sufficient attraction by the neighbors.

At $C \approx 0.005$ the correlations of the magnetic moments vanish, and the magnetic and nuclear dimensions become comparable within the limits of error. We have pointed out above the change in the character of the cross section behavior at these concentrations. This can apparently be explained by the described structural singularities. It can be seen from (8) and (9) that the cross sections depend on the product

$V^2 N$. If the particles stick together, the cross section is increased by the stronger increase of the factor V^2 compared to the weak decrease of N .

3. Inelastic scattering

The magnetic dynamics of the liquids is indicated by the scattering inelasticity observed by us. As mentioned in Sec. 2, in inelastic magnetic small-angle scattering the polarization component P_{mz} is not zero. Averaged over the spectrum of the scattered neutrons and normalized to P_{0z} , it takes the form²²

$$P_{mz} = - \left(\int d\omega \frac{d^2 \sigma_m}{d\Omega d\omega} \right)^{-1} \int d\omega \frac{\omega^2}{4E^2} \left(\frac{1}{\theta^2 + \omega^2/4E^2} \right) \frac{d^2 \sigma_m}{d\Omega d\omega}, \quad (12)$$

where ω is the energy transferred in scattering, θ the scattering angle in the YZ plane,³⁾ E the initial neutron energy, and $d^2 \sigma_m / d\Omega d\omega$ the doubly differential cross section for magnetic scattering.

If the energy ω is low compared with E and if $\omega/2E \ll \theta$, we have

$$P_{mz} = - \overline{\omega^2} / 4E^2 \theta^2, \quad (13)$$

where $\overline{\omega^2}$ is the mean squared characteristic energy of the distribution.

Figure 8 shows for the four most concentrated ML the components P_{mi} , with P_{mx} and P_{my} responsible for the elastic scattering. The components are noticeable only in the range of q where the magnetic scattering is still appreciable. The component P_{mz} is small in dilute FL, and only in a strongly concentrated FL does it reach a level ~ 0.5 . Table I lists by way of estimates the values of $\langle \overline{\omega^2} \rangle_q^{1/2}$, obtained by averaging P_{mz} over the interval q in accordance with (13).

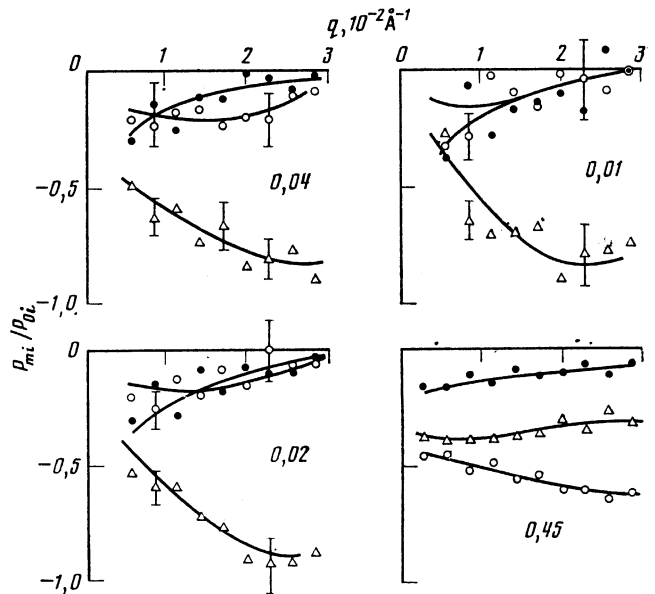


FIG. 8. Magnetic-scattering polarization components P_{mi}/P_{0i} (\bullet — P_{mx} , Δ — P_{my} , \circ — P_{mz}) for the concentrations marked by the numbers on the figures.

averaging P_{mz} over the interval q in accordance with (13).

The characteristic times corresponding to these energies are of the order of $5 \cdot 10^{-11}$ s. To what processes do these times correspond? It is difficult to give an unambiguous answer. On the one hand, they are of the same order of magnitude as the so-called "viscous" time²⁴ that characterizes the density relaxation rate of the internal angular momentum of a suspension as a result of the intrinsic rotation of the particles:

$$\tau_s = I_0 / 6\eta V,$$

where I_0 is the sum of the particle moment of inertia per unit volume, η is the viscosity of the medium, and V is the particle volume.

On the other hand, in magnetodipole interaction the particle moments exchange an energy U_d within times $\tau \approx \hbar / U_d \approx 10^{-12}$ s (the dipole energy for $C = 0.04$ is $U_d \approx mH_i \approx 6 \cdot 10^{-15}$ erg) that are shorter than the interaction time ($\sim 10^{-11}$ s) than the interaction time of the neutron with a magnetic inhomogeneity of size $d_m \approx 200$ Å. Consequently, the neutron should "feel" the motion of the moments. It is possible that the time $\tau \approx 5 \cdot 10^{-11}$ s characterizes the relaxation of the particle's magnetic moment when the particle alters its environment in sufficiently concentrated liquids, where the particles are closely crowded and their moments change orientation frequently under the influence of the thermal motion and of the field produced by neighbors. At low concentrations (0.0025), where stable formation in the form of particles that have stuck together exist, the scattering is elastic.

In conclusion, we are grateful to S. V. Maleev, B. P. Toperverg, A. I. Okorokov, V. V. Runov, E. E. Bibik, and M. I. Shliomis for a discussion of the work, critical remarks, and advice. We thank N. M. Gribanov for preparing the samples, and B. M. Kholkin, V. P. Grigor'ev, V. V. Lepekhin, M. R. Kolkhidashvili, and I. V. Maninen for technical help with the experiment.

¹¹An extensive bibliography on magnetic liquids, including patents, is contained in Ref. 1.

²⁰We are treating scattering in the quasi-elastic approximation, so that $q = k_0\theta$ everywhere.

³¹Generally speaking, Eq. (12) should contain the effective scattering angle θ_{eff} , in view of the presence of a vertical divergence of the beam. However, even for a quadratic dependence of the scattering intensity on the angle ($I_m \propto \theta^{-2}$) the correction for the vertical divergence is small.²³ In our case $I_m \propto \theta^{-4}$ and is therefore disregarded.

¹S. W. Charles and R. E. Rosensweig, *J. Magn. Magn. Mater.* **39**, 190 (1983).

²L. F. Hayes and S. R. J. Hwang, *J. Coll. Inter. Sci.* **60**, 443 (1977).

³R. Anthere, C. Petipas, D. Chandersis, and A. Martinet, *J. Phys. Colloq.* **38**, C2-203 (1977).

⁴E. A. Peterson and D. A. Kruger, *J. Coll. Inter. Sci.* **62**, 24 (1977).

⁵D. J. Cebula, S. W. Charles, and J. Popplewell, *J. Physique* **44**, 297 (1983).

⁶D. J. Cebula, S. W. Charles, and J. Popplewell, *J. Phys.* **F12**, L229 (1982).

⁷L. F. Hayes, *Coll. Inter. Sci.* **52**, 239 (1975).

⁸P. C. DeGennes and P. A. Pincus, *Phys. Kondens. Mater.* **11**, 189 (1970).

⁹E. E. Bibik, *Magn. Gidrodinamika* **3**, 25 (1973).

¹⁰P. C. Jordan, *Molec. Phys.* **25**, 961 (1973).

¹¹P. C. Jordan, *ibid.* **38**, 769 (1979).

¹²K. Sano and M. Doi, *J. Phys. Soc. Jpn.* **52**, 2810 (1983).

¹³R. W. Chantrell, A. Bradbury, J. Popplewell, and S. W. Charles, *J. Phys.* **D13**, L119 (1980).

¹⁴I. N. Gurevich and L. V. Tarasov, *Physics of Low-Energy Neutrons* [in Russian], Nauka, 1965, p. 580.

¹⁵O. Halpern and M. H. Johnson, *Phys. Rev.* **55**, 898 (1939).

¹⁶V. E. Mikhailova, L. A. Aksel'rod, G. P. Gordeev, A. G. Gukasov, I. M. Lazebnik, V. T. Lebedev, A. I. Okorokov, V. V. Rukov, and V. N. Slyusar, Preprint LIYaF-696, 1981.

¹⁷S. V. Maleev and V. A. Ruban, *Zh. Eksp. Teor. Fiz.* **62**, 415 (1972) [*Sov. Phys. JETP* **35**, 222 (1972)].

¹⁸G. P. Gordeev, I. M. Lazebnik, and L. A. Aksel'rod, *Fiz. Tverd. Tela* (Leningrad) **18**, 2059 (1976) [*Sov. Phys. Solid State* **18**, 1198 (1976)].

¹⁹A. Guinier and G. Founet, *Small-Angle Scattering of X Rays*, Wiley, 1955, p. 24.

²⁰G. Porod, *Kolloid Z.* **124**, 83 (1951); **125**, 51, 109 (1952).

²¹S. V. Maleev, *J. Physique* **43**, C7-23 (1982).

²²Maleev, *Pis'ma Zh. Eksp. Teor. Fiz.* **2**, 545 (1965) [*JETP Lett.* **2**, 338 (1965)].

²³V. V. Runov, A. I. Okorokov, and A. G. Gukasov, Preprint LIYaF-507, 1979.

²⁴M. I. Shliomis, *Usp. Fiz. Nauk* **112**, 427 (1974) [*Sov. Phys. Usp.* **17**, 153 (1974)].

Translated by J. G. Adashko